Oxygen-Rich Carbon Quantum Dots as Catalysts for Selective Oxidation of Amines and Alcohols

Jianglin Ye,[a] Kun Ni,[a] Jie Liu,[a] Guanxiong Chen,[a] Mujtaba Ikram,[a] and Yanwu Zhu*[a, b]

Metal-free carbocatalysis has been widely utilized for aerobic oxidative reactions. Here, we report that oxygen-rich carbon quantum dots (O-CQDs) demonstrate a catalytic performance superior to graphene oxide, if used as a metal-free nanocatalyst for the direct transformation of amines and alcohols, under mild and solvent-free conditions. O-CQDs show a yield of 75% for the oxidative coupling of amine to imine (with 5 wt% catalyst loading) and a conversion of 3.8% for benzyl alcohol (with 2 wt% catalyst loading). The catalytic activities of thermally treated O-CQDs are further improved for benzylamine, for example, indicated by a yield of up to 98% with 4 wt% catalyst loading. In addition, O-CQDs show a photoenhanced catalytic ability of amine (98% yield with 5 wt% catalyst loading for 6 h reaction). Characterizations and simulations show that numerous carboxyl oxygen functional groups and unpaired electrons at the edge sites of O-CQDs are likely involved in the aerobic oxidation of amines.

Introduction

Catalytic oxidation of chemicals by using oxygen molecular as an oxidant for high-quality products remains a significant challenge in fine chemical processes and green chemistry.[1] Compared with traditional metal-based catalysts, carbon-based materials, including graphene oxide, carbon nanotubes, amorphous carbon, mesoporous carbon, and graphitic carbon nitride, have been developed as potential catalysts owing to their relatively low cost and good natural abundance.[2] In many heterogeneous oxidation reactions, carbon materials serve both as supporting scaffolds for metal catalysts as well as carbocatalyst in its own right. Among the potential carbocatalysts, graphene oxide (GO) produced by exfoliation of graphite oxide has been investigated for the oxidation of alcohols,[3] alkanes,[4] and amines.[5] The oxygen-containing functional groups and rich defects in the carbon backbone of GO provide active sites to trap and activate target molecular species.[6] In addition, the conjugated π-electron system leads to the co-existence of both aromatic and olefin properties in graphene-based catalysts.[7] The high catalyst loading (typically 20–400 wt%) for typical oxidative reactions, however, hinders the further application of GO-based catalysts.[3a]

With a typical size below 10 nm, carbon quantum dots (CQDs), including graphene quantum dots (GQDs), have exhibited unique physical and chemical properties, and found applications in catalysis and bio-imaging.[8] Previous works have demonstrated that CQDs decorated with hydrogen sulfate groups give a new aspect in enhanced photocatalyzed performance for the ring-opening of epoxides.[9] With photoluminescence (PL) and photoinduced electron transfer/reservoir properties, CQDs have been used as heterogeneous catalysts for hydrogen-bond catalysis, showing excellent photoenhanced catalytic abilities with a yield of 89% in the aldol condensation if 4-cyanobenzaldehyde was used as reactant.[10] Hybrids of CQDs and semiconductors were also prepared, demonstrating further improved photocatalytic activities.[11] For example, CQD modified MoS_2 has been explored in the catalysis of the hydrogen evolution reaction (HER) under visible light,[12] and the improved HER activity has been ascribed to the high charge transfer efficiency between CQDs and MoS_2. Relatively, there are few reports demonstrating aerobic oxidation reactions by using CQDs. The abundant edge active sites and rich photochemical properties owing to the quantum size effect in CQDs have prompted us to investigate the possibility of using oxygen-functionalized CQDs for direct transformation of reactants by aerobic oxidation. However, the typical content of oxygen-containing functional groups in CQDs cannot reach that of GO.[13]

Herein, we present a detailed study on the catalytic performance of oxygen-rich carbon quantum dots (O-CQDs) as metal-free nanocatalyst for the aerobic oxidation of amines and alcohols. With oxygen-containing functional groups and possible curvatures owing to the presence of pentagons, O-CQDs have demonstrated excellent catalytic abilities for the selective oxidation of alcohols to aldehyde; a yield of up to 98% has also been obtained with a relatively low catalyst loading

[a] J. Ye, K. Ni, J. Liu, Dr. G. Chen, M. Ikram, Prof. Y. Zhu
Key Laboratory of Materials for Energy Conversion
Chinese Academy of Sciences &
Department of Materials Science and Engineering
University of Science and Technology of China
Hefei, Anhui, 230026 (P.R. China)
E-mail: zhuyanwu@ustc.edu.cn

[b] Prof. Y. Zhu
iChEM (Collaborative Innovation Center of Chemistry for Energy Materials)
University of Science and Technology of China
Hefei, Anhui, 230026 (P.R. China)

⌨ Supporting information for this article can be found under:
https://doi.org/10.1002/cctc.201701148.

(4 wt%) for the oxidative coupling of amine to imine under mild conditions (90 °C and solvent-free). It is suggested that numerous carboxyl oxygen functional groups coupled with the spins of π-electrons from the atoms located at the edge sites of O-CQDs are most likely involved in the aerobic oxidation of amines. In addition, photoinduced electron acceptance in O-CQDs has led to further improvement in the efficient catalytic oxidation performance of amines under light illumination.
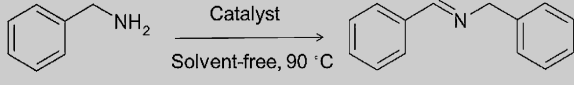
Results and Discussion

O-CQDs were prepared from fullerenes (C_{60}) by using a modified Hummers' method and the preparation is described in the Supporting Information and our previous report.[14] To ensure the removal of metallic residuals, the as-obtained O-CQD suspension was dialyzed for 8 days before the catalysis studies. The content of Mn, Fe, and SO_4^{2-} in the dialyzed suspension was all found to be lower than 10 ppm based on inductively coupled plasma mass spectrometry (ICP-AES) analysis. The typical diameter of O-CQDs falls in the range 0.6–2.2 nm with an average height of approximately 1.2 nm (Figure S1 in the Supporting Information). The Raman spectra of O-CQDs clearly show the presence of the G band (≈ 1580 cm^{-1}) and D band (≈ 1360 cm^{-1}) of graphitic carbon (Figure S2 in the Supporting Information). The Raman band near 1470 cm^{-1} may be ascribed to the Ag(2) vibration mode of pentagon pinch remaining in the O-CQDs. A broad PL peak through a down-conversion process was observed from O-CQDs;[15] the PL intensity increases with excitation wavelength for excitation wavelengths lower than 360 nm, then decreases with excitation wavelength for longer excitation wavelengths (Figure S2 in the Supporting Information).

We focus on the oxidative coupling of amines to form imines, which are important electrophilic intermediates in organic synthesis.[16] As shown in Table 1, performing oxidation reactions by using O-CQDs as the catalyst and oxygen as the oxidant under mild conditions (90 °C and solvent-free) resulted in a high yield for N-benzylidene benzylamine. The conversion is lower than 0.5% in the absence of catalyst (Table 1, entry 1). The variations in the O-CQDs loadings and reaction times have significant impacts on the yield of the imine product (Table 1, entries 2–5). For the O-CQDs catalyst loadings below 2 wt%, the reaction exhibits a first-order rate dependence with respect to amine with a rate constant of 0.029 h^{-1} (Figure S3 in the Supporting Information).[17] Higher concentrations of catalyst and longer reaction duration resulted in significantly improved catalysis performance. Compared with GO and multiwalled carbon nanotube (MWCNT) catalysts, O-CQDs show a much higher yield under the same conditions, indicated by, for example, a yield of 75% for O-CQDs, remarkably higher than that of 47% for GO and that of 6% for MWCNTs for the same catalyst loading of 5 wt% (Table 1, entries 5, 7, and 8).

In addition, it has been reported that light-induced electrons (e$^-$) can activate molecular oxygen during the synthesis of organic compounds.[10,18] Thus, the oxidative reaction was also conducted under irradiation of visible light by using the O-CQD catalyst; a notable yield of up to 98% for the oxidation of

Table 1. Oxidation of benzylamine to N-benzylidene benzylamine.[a]

Entry	Catalyst	Loading [wt%]	Yield [%]
1	no catalyst	–	< 0.5
2[b]	O-CQDs	2	14
3	O-CQDs	2	31
4[c]	O-CQDs	2	43
5	O-CQDs	5	75
6	GO	2	21
7	GO	5	47
8	MWCNTs	5	6
9[d]	O-CQDs (hv)	2.5	54
10[d]	O-CQDs (hv)	5	98
11	RO-CQDs	5	7
12	O-CQDs (N$_2$)	5	5
13	HO-CQDs	2	54
14	HO-CQDs	4	98
15[d]	HO-CQDs (hv)	2	56
16[e]	porous-GO	5	98
17[f]	Au/Al$_2$O$_3$	5	92

[a] Standard reaction conditions: 25 mg catalyst, 90 °C under solvent-free and oxygen conditions for 12 h. Catalyst loading wt% is the ratio of weight of catalyst to that of amine. [b,c] Reaction was run under the standard conditions but for [b] 6 h and [c] 20 h, respectively. [d] Reactions were run under the standard conditions but for 6 h with visible light irradiation. [e] Ref. [5b]. [f] Ref. [19]. Yield percentage was calculated by using ^{1}H NMR spectroscopy.

amine to imine is obtained with 5 wt% catalyst loading for a 6 h reaction (Table 1, entry 10), higher than those from 5 wt% O-CQDs (Table 1, entry 5) or 5 wt% GO (Table 1, entry 7) measured under the same conditions except without irradiation. No observation of enhanced catalytic ability in the oxidative coupling of amines to form imines under visible light irradiation has been previously reported for heterogeneous aerobic oxidation by using GO-based catalysts. Control experiments, performed in a nitrogen atmosphere or by using reduced carbon quantum dots (named RO-CQDs, obtained by annealing O-CQDs at 800 °C for 2 h in Ar) with much less amount of oxygen functional groups as catalysts (Figure S4 in the Supporting Information), show dramatic decreases in the yield (Table 1, entries 11 and 12). The results indicate that oxygen is the terminal oxidant and the major catalytically active sites are lost in RO-CQDs. To further investigate the contribution of oxygen functional groups in the catalyst, O-CQDs was gently reduced by heating at 200 °C, resulting in a sample named as HO-CQDs in which some oxygen functional groups, such as C-O, are partially removed. As shown in Table 1, entry 14, HO-CQDs surprisingly show an improved conversion of 98% from amine to imine, with a catalyst loading of 4 wt%. Such a conversion efficiency from HO-CQDs is higher than that from porous GO catalyst (5 wt% loading, 98% yield, 12 h, entry 16) or from Au/Al$_2$O$_3$ (5 wt% loading, 92% yield, 24 h, entry 17). The recyclability of HO-CQDs was tested by repeatedly using the catalyst recycled by filtration and rinsed in acetonitrile. As shown in Figure 1, HO-CQDs show a good recyclability and the decrease in yield with recycle number is not significant for five
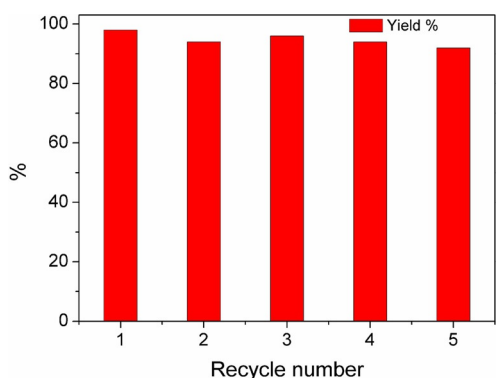
Figure 1. Recyclability of HO-CQDs in benzylamine oxidation. Reaction conditions: 90 °C, oxygen condition, 4 wt % catalyst loading, 12 h.

cycles. To summarize, the performance of as-made O-CQDs is superior to that of the GO catalyst; the catalytic activity of the HO-CQDs catalyst and photocatalytic activity of O-CQDs are comparable or even superior to those of porous GO, doped carbon catalysts, or metal catalysts.[5b, 16a, 19]

The oxidation of different types of amines is explored by using O-CQDs as the catalyst. It is proven that benzylamines with the electron-donating methyl groups are suitable substrates (Table 2, entries 1 and 2). If 4-chlorobenzylamine was used as the reactant, with an electron-withdrawing group, an imine yield of 91 % was obtained (Table 2, entry 3). The catalyst was also applicable for the oxidation of 2-thiopheneamine, containing S as heteroatom (Table 2, entry 4), indicating a high toleration for electronic effects of the substituents on the phenyl ring under mild reaction conditions.[5b] The Hammett plot can be obtained by the oxidation of benzylamine and its derivatives with *para*-position substituents (Figure S5 in the

Supporting Information),[20] suggesting that the oxidation is favored by the presence of electron-donating substituents. However, the oxidation of aniline lacking α-H atoms did not proceed at all (Table 2, entry 5). O-CQDs can also be used to synthesize unsymmetrical imines by the oxidative cross condensation of benzylamines and amines. Reactions between aniline and benzylamine were performed at different conditions (Table 2, entries 6–9). The reaction with 4:1 molar ratio of aniline/benzylamine exhibited a yield of 23 % towards the unsymmetrical imine. The rate of the reaction can be further improved under visible light irradiation (Table 2, entry 8).

To determine why O-CQDs, especially HO-CQDs show catalytic properties superior to GO for the oxidative coupling of amines to imines, the detailed chemical bonding configuration was investigated by using thermogravimetric analysis (TGA) and X-ray photoelectron analysis (XPS). Figure 2 a shows TGA
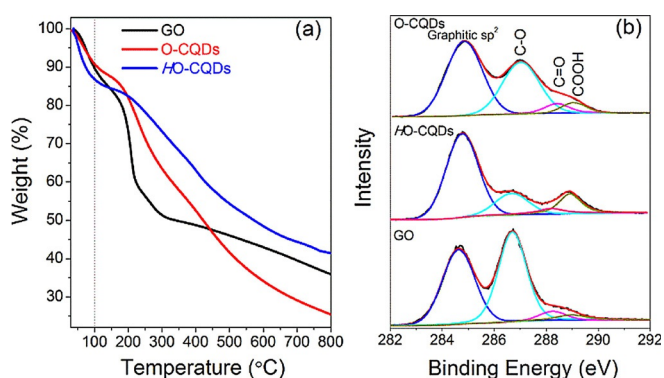

Figure 2. (a) Thermogravimetric analysis of O-CQDs, GO, and HO-CQDs. (b) XPS C 1s spectra of O-CQDs, GO, and HO-CQDs, respectively.

thermograms of O-CQDs, HO-CQDs, and GO obtained in a nitrogen atmosphere. About 10 % weight loss is found for both O-CQDs and GO below 100 °C, which accounts for the volatilization of water molecules. In comparison, HO-CQDs show a slightly higher weight loss (14 %) below 100 °C, indicating the stronger hygroscopic nature in HO-CQDs. Compared with GO, a much lower weight loss between 100 and 400 °C is shown from O-CQDs and HO-CQDs, suggesting more pyrolysis of the labile oxygen-containing groups present in GO. The residual weight of GO retains 36 % of its initial mass at 800 °C whereas that of O-CQDs sharply decreased to only 26 % under the same conditions. HO-CQDs show less weight loss than O-CQDs and GO at 800 °C. These results reveal that the concentration of oxygen functional groups in O-CQDs is more than that in GO and some unstable oxygen functional groups have been effectively removed in HO-CQDs. The high-resolution C 1s peaks are shown in Figure 2 b and C/O in different groups are obtained from the deconvolution (Table 3). The deconvolution of the C 1s peak for all three catalysts shows a similar type of oxygen functional groups. Four main carbon bonding types: C—C (≈ 284.7 eV), C—O (≈ 286.9 eV), C=O (≈ 288.4 eV), and COOH (≈ 288.9 eV) can be ascribed.[21] The C/O atomic ratio obtained from XPS is 1.2 for O-CQDs, less than that of 1.7 for the GO catalyst or 2.2 for HO-CQDs. Further analysis shows that 35.8 %

Table 2. Oxidative coupling of primary amines to imines catalyzed by O-CQDs.[a]

Entry	Substrates	t [h]	Yield [%]
1[b]	(4-methylbenzylamine)	10	85
2[b]	(2-methylbenzylamine)	10	81
3[b]	(4-chlorobenzylamine)	12	91
4[b]	(2-thiophenemethylamine)	12	64
5[b]	(aniline)	20	–
6[c]		8	**1**: 4 / **2**: 96
7[d]	(aniline + benzylamine)	6	**1**: 23 / **2**: 77
8[d]		4 ($h\nu$)	**1**: 25 / **2**: 75
9[d]	(aniline + 4-chlorobenzylamine)	6	**1**: 29 / **2**: 71

[a] Standard reaction conditions: 90 °C under solvent-free and oxygen conditions. [b] 5 wt % loading of O-CQDs. [c] 1 mmol aniline, 1 mmol benzylamine, 10 mg of O-CQDs. [d] 4 mmol aniline, 1 mmol benzylamine, 20 mg of O-CQDs.

Table 3. Fraction of elements in various chemical bondings obtained from the deconvolution of the C 1s peak.

Entry	O-CQDs	HO-CQDs	GO	H-GO
total carbon (C)	53.8	68.7	63.2	80.2
total oxygen (O)	46.2	31.3	36.8	19.8
oxygen in C—O	35.8	15.8	30.9	12.4
oxygen in C=O	5.1	3.1	3.2	1.5
oxygen in COOH	5.3	12.4	2.7	5.9

of the total oxygen is in the form of C—O and 5.3% in the form of COOH for O-CQDs, both higher than the case in GO (30.9% of C—O and 2.7% of COOH). The fraction of COOH is 12.4% in HO-CQDs. For comparison, GO was also gently reduced by heating at 200°C (leading to a sample named H-GO). The C/O atomic ratio obtained from XPS is 4.1 for H-GO, and the fraction of COOH increases to 5.9% in H-GO (Table 3 and Figure S6 si). Interestingly, H-GO has shown an improved yield (80%) for *N*-benzylidene benzylamine if compared with that of GO (47%, seen in Table S1 in the Supporting Information) for the same loading of 5 wt%. According to a previous report,[22] hydroxyl groups have lower decomposition temperatures (100–150°C) compared with carboxyl and ketones; the thermal treatment at 200°C gives rise to the quick decomposition of hydroxyl, leading to a relatively improved percentage of carboxyl.

Fourier transform infrared spectroscopy (FTIR) and ^{13}C solid-state NMR spectra (Figure S7 in the Supporting Information) were performed to further analyze the functional groups in O-CQDs, GO, and HO-CQDs. As previously reported,[5b,22,23] infrared spectra of all types of catalysts indicate contributions from various oxygen functional groups. Vibrational modes are shown for hydroxyls (C—OH, ≈3000–3700 cm^{-1}), C—H$_x$ (≈2800–3000 cm^{-1}), carboxyls and/or ketones within an overlapped frequency range (C=O, COOH, ≈1700–1900 cm^{-1}), sp^2-hybridized C=C (≈1550–1650 cm^{-1}), epoxides (C-O-C, 1100–1400 cm^{-1} and 800–900 cm^{-1}), and ethers (C—O, 800–1200 cm^{-1}).[24] In contrast to GO, O-CQDs possess stronger epoxides (O—C—O), C—O, and C—OH. However, the intensity of the carboxyl peak in O-CQDs is lower than that in HO-CQDs. In addition, C—H$_x$ stretching is almost eliminated by the annealing, indicating the further exposure of carbon edges. ^{13}C NMR spectra of O-CQDs and HO-CQDs reveal a broad resonance peak at 138.0 ppm, which suggests sp^2 conjugation. The oxygen signals at 73.4 ppm (C—OH) are largely deteriorated in HO-CQDs, which is consistent with the XPS results. In observation of the fact that HO-CQDs and H-GO demonstrated higher conversion efficiencies in the oxidation of amine compared with O-CQDs and GO, respectively, the spectroscopic results provide strong evidence that the carboxylic acid group plays an important role in the aerobic oxidation of amines.

According to the Lerf–Klinowski model,[25] epoxy and hydroxyl groups mainly reside on the O-CQDs basal plane, whereas the periphery of the O-CQDs sheets is mainly decorated by carboxyl and anhydride groups. In addition, the carboxylic groups in porous GO have been considered as the active group, which serve as hydrogen-bonding sites for the oxidation of amine.[5b] The carboxyl-rich nature and nanoscale feature of O-CQDs and HO-CQDs make them have more catalytically active edge sites (Figure S8a in the Supporting Information). In addition, it has been found that the molecules with both carboxylic acid groups and large π-conjugation, for example, 1-pyrene carboxylic acid, can exhibit high reactivity in the oxidative coupling of benzylamine; the carboxylic acids without large π-conjugation did not exhibit catalytic activity.[5b] 1-Pyrene carboxylic acid has been used as a molecular analog of the CQDs made in this work (Figure 3a). Compared with GO, the much smaller
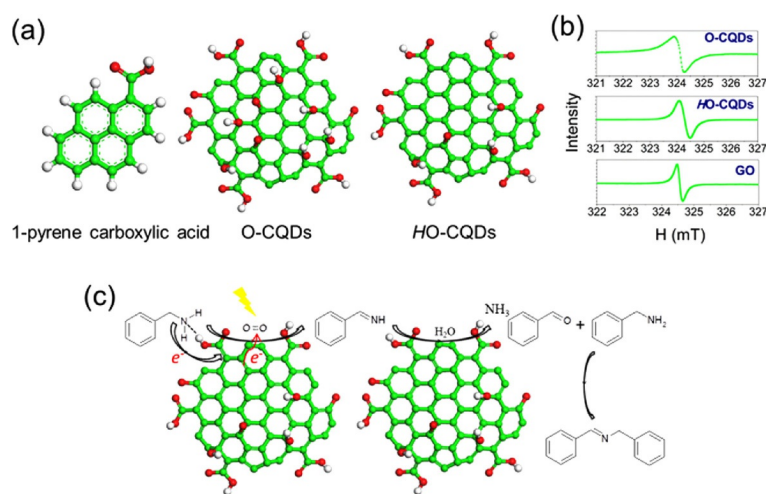

Figure 3. (a) Structure schematic of 1-pyrene carboxylic acid, O-CQDs, and HO-CQD. (b) EPR measurements of O-CQDs, HO-CQDs, and GO. (c) A proposed reaction process over O-CQDs.

size of O-CQDs results in more periphery area, which is surrounded by conjugated carbons; electron spins originating from the non-bonding π electron states are found at the active edges (simulation results in Figure S8b,c in the Supporting Information).[26] EPR investigations (Figure 3b) have shown that the concentration of spins is about 1.9×10^{18} spins g^{-1} for O-CQDs, 2.4×10^{19} spins g^{-1} for HO-CQDs, which are both more than 100 times higher than that of GO (8.2×10^{16} spins g^{-1}). In addition, unpaired electrons may be highly reactive towards the coupling of diazonium.[27] We functionalized O-CQDs with phenyl groups by using diazonium coupling reactions, leading to a sample named as O-CQDs-Ph (Figure S9 in the Supporting Information). The catalytic activity of O-CQDs-Ph has been reduced to 21% from 32% for as-prepared O-CQDs in the oxidative coupling of benzylamine, suggesting that the high catalytic ability in O-CQDs and HO-CQDs are related to the unpaired π-electron.

The unpaired electrons of CQDs may have activated oxygen molecules during the oxidation reactions.[5b,28] According to the literature on metal-free carbocatalysis using oxygen molecular as the oxidant,[5a,29] it is believed that an oxidative dehy-

drogenation involving the formation of RCH=NH intermediates could be the key for achieving highly efficient amine oxidation.[19a,30] It was found that a free-radical scavenger (butylated hydroxytoluene, BHT) could not quench the oxidation of benzylamine (Table 4, entry 1), revealing that O_2 is activated direct-

Table 4. Oxidative coupling of amine catalyzed by O-CQDs in the presence of a radical quencher and deionized water, respectively.
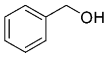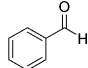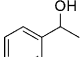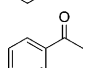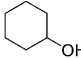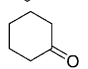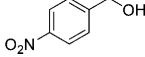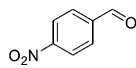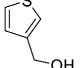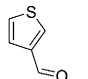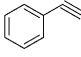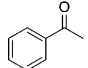
Entry	Substrate	Yield [%]
1[a]	benzylamine (with BHT)	32
2[b]	benzylamine (with H_2O)	58

Reaction conditions: 2 wt% of O-CQDs catalyst, 90 °C, 12 h. [a] 200 wt% of BHT was added. [b] 2 mmol H_2O was added.

ly on the surface of the catalyst for the oxidation reactions.[16a] Interestingly, the conversion efficiency can be enhanced if some amount of H_2O was introduced at the beginning of the reaction (Table 4, entry 2). TGA results also show the stronger hygroscopic nature of HO-CQDs, indicating that the amount of H_2O plays an important role in the aerobic oxidation. In addition, ammonia was also detected in the oxidation reaction. Based on these observations, a reaction path is proposed and shown in Figure 3c. The formation of aminal intermediate reacts with H_2O and loses NH_3 to produce aldehyde RCH=O; the aldehyde subsequently reacts with a second amine molecule to give the final imine coupling product. In addition, if the reactions were conducted under light irradiation, the conversion efficiency was further improved, indicating that the extra electrons generated in carbon dots further activate oxygen molecules for the reaction (Figure S10 in the Supporting Information).[31] The heterogeneous oxidation caused by the edges of defects and photoinduced electrons work synergistically to trap amine molecules and activate molecular oxygen, thus improving the conversion efficiency of O-CQDs.

Meanwhile, the catalytic efficiency of O-CQDs for solvent-free aerobic selective oxidation of alcohols with different catalyst loadings was investigated (Table 5). For the reactions, neat alcohols were heated up to the given temperature in the presence of various wt% O-CQDs, under 1 atm of oxygen. For 2 wt% O-CQDs loading, the conversion is about 3.8% with a turnover number (TON) of 1.9×10^{-2} to benzaldehyde (Table 5, entry 1). In addition, the conversion percentage for the O-CQDs catalyst was found to increase from 1.7% to 6.2% with reaction time for 1 wt% catalyst loading (Table S2 in the Supporting Information). It is worth noting that the catalytic efficiency of O-CQDs is much higher than that of GO (Figure S11 in the Supporting Information) under the same reaction conditions. No benzoic acid was found in these reactions. On the other hand, reduced O-CQDs (RO-CQDs) were found to be unreactive (Table S2, entries 8 and 9 in the Supporting Information), and HO-CQDs resulted in negligible conversion (Table S2, entry 10 in the Supporting Information). From the XPS and NMR spectra (Figure S7 in the Supporting Information), the loss of oxygenated groups such as C—OH may cause the de-

Table 5. Catalytic activity of O-CQDs in the oxidation on different alcohols.[a]

Entry	Substrate	Product	Conversion [%]
1[b]	benzyl alcohol	benzaldehyde	3.8
2[c]	1-phenylethanol	acetophenone	6.7
3[c]	cyclohexanol	cyclohexanone	8.4
4[d]	4-nitrobenzyl alcohol	4-nitrobenzaldehyde	ND
5[e]	3-thiophenemethanol	3-thiophenecarbaldehyde	3.5
6[f]	phenylacetylene	acetophenone	5.6

[a] Standard reaction conditions: 25 mg catalyst, different weights of different alcohols to make different wt% of catalyst, 1 atm O_2. [b] Reactions were performed at 100 °C for 48 h by using 2 wt% O-CQDs. [c] Reactions were performed at 100 °C for 24 h by using 2 wt% O-CQDs. [d] Reaction was performed at 90 °C for 48 h by using 2 wt% O-CQDs. [e] Reaction was performed at 75 °C for 12 h by using 2.5 wt% O-CQDs. [f] Reaction was performed at 100 °C for 24 h by using 4 wt% O-CQDs. ND = not determined.

crease in the active sites in HO-CQDs. Therefore, when primary benzyl alcohol was used as a reactant, the condensation was likely facilitated by the interaction of the alcohol with the polar groups (such as C—OH, O—C—O) on O-CQDs by hydrogen bonding.[32] Our results indicate the sensitivity depends on the type of surface functional groups in CQDs for the selective oxidation reaction of alcohols and amines. Furthermore, the reactions of α-phenylethanol and cyclohexanol show similar conversion efficiencies under same conditions, which is higher than that of benzyl alcohol (Table 5, entries 2 and 3). However, the -NO_2 substituted functional groups attached to the aromatic ring of benzylic alcohols results in a negligible conversion (Table 5, entry 4), and a modest conversion of 3-thiophenemethanol into the respective aldehyde without sulfur oxidation is obtained (Table 5, entry 5). Moreover, a treatment of O-CQDs with alkyne afforded its respective ketone product, which furthermore indicates the ability to oxidize unsaturated hydrocarbons by O-CQDs catalysts (Table 5, entry 6). The results indicate that O-CQDs may exhibit broad chemoselectivity.

Conclusions

We demonstrated that O-CQDs can be used as selective metal-free catalysts for the aerobic oxidation of amines and alcohols without using any solvents. Based on studies on the reaction process of the oxidative coupling of amines to form imines, it is proposed that the carboxylic groups at the edges of the carbon dots, along with the unpaired electrons, work synergistically to trap and activate molecular oxygen and the amine molecules, thus facilitating the conversion of amine. Heat treat-

ment has further improved the catalytic activities of O-CQDs for oxidative coupling of amine to imine because of the increase in both active sites and unpaired electrons. The mild synthetic procedure and unprecedentedly low catalyst loading described herein is expected to find utilization in metal-free catalysis for a wide range of solvent-free oxidations.

Experimental Section

Preparation of O-CQDs

The oxygen-rich carbon quantum dot (O-CQD) powder was first synthesized by a modified Hummers' processing of C_{60} as described in a previous report.[14] Briefly, fullerene (500 mg, 99.9%, XF NANO, Inc.) was mixed with concentrated H_2SO_4 (25 mL) and cooled in an ice water bath. Under vigorous stirring, $KMnO_4$ (1.75 g, 99.6%) was added gradually, and the temperature of the mixture was kept below 5 °C. The mixture was stirred at 25 °C in a water bath for another 24 h after removing the ice bath. H_2O (150 mL) was slowly added to the pasty mixture to get a deep-yellow solution. The mixture solution was then purified by dialysis for 8 days. Finally, the resulting solution was dried by freeze-drying to get the O-CQDs powder. RO-CQDs, HO-CQDs, and H-GO were prepared by a simple heat treatment at 800 °C or 200 °C for 2 h in argon, respectively. The GO powder was prepared from natural graphite powder by using a Hummers' method.[33] Multiwalled carbon nanotubes (MWCNTs) with diameters of 30–50 nm were obtained from Chengdu Organic Chemicals Co., Ltd. and used without further treatment.

Solvent-free synthesis of imines

In a typical reaction, after mixing benzylamine with the specified amount of catalyst (as mentioned in Tables 1 and 2, the catalyst loading is the ratio of weight of catalyst to that of amine) the mixture was ultrasonicated for 10 min, the reactor was sealed in the desired atmosphere and heated in an oil bath at the predetermined temperature for certain reaction durations. After the reaction, the mixture was further mixed with $CDCl_3$ ($\approx$0.7 mL), filtered through 20 nm PTFE filter membrane to remove the catalyst before analysis by ^1H NMR spectroscopy. Butylated hydroxytoluene (BHT) or H_2O was added to the above-described mixture at the beginning of the reaction. For the recycle experiments, HO-CQDs and O-CQDs were separated from the reaction mixture by vacuum distillation to remove the reactants, products, and solvents. However, approximately 20 wt% of the O-CQDs catalyst cannot be recovered because of the smaller sizes. Approximately 95 wt% of HO-CQDs catalyst can be recovered. To carry out the photochemical reaction (hv), a 300 W xenon lamp together with a 420 nm cut-off filter was used as a visible light source for the irradiation of the reaction system. All reactions were performed under complete darkness except in the control experiments of light irradiation.

Representative oxidation procedure of alcohols

A Teflon-line (25 mL, stir bar) reactor was charged with 25 mg of catalysts and different weights of alcohol. After ultrasonication for 10 min, the reactor was sealed and purged with oxygen and then heated to the given temperature. After the reaction was completed, the solution was cooled to room temperature, filtered, and vacuum distillated to remove the catalyst, and then analyzed by

NMR spectroscopy. The turnover number (TON) was calculated as the molar ratio of the oxidized product to mass of catalyst.

Characterizations and simulation

Thermogravimetric analysis (TGA) was performed by using a Q50000 IR (TA, US) in nitrogen for temperatures rising from room temperature to 850 °C with a step of 10 °C min^{-1}. Transmission electron microscopy (TEM) images and high-resolution (HR)TEM images were taken with a JEM-ARM200F (JEOL, Japan). Atomic force microscopy (AFM) images were obtained from an AFM (Nanoscope Icon, Veeco) at room temperature. Raman spectra were collected by using an inVia Raman microscope (Renishaw, 532 nm laser, UK). Inductively coupled plasma atomic emission spectrometry (ICP-AES) was performed by using an Optima 7300 DV (PerkinElmer, US). X-ray photoemission spectroscopy (XPS) was performed with a Thermo ESCALAB 250 (Thermo Scientific, US) with AlK_α radiation ($hv = 1486.6$ eV). Fourier transform infrared spectroscopy (FTIR) was performed by using a Nicolet 8700 (Thermo Scientific, US). Electron paramagnetic resonance (EPR) spectra were obtained by using a JES-FA 200 (JEOL, Japan). ^1H NMR spectroscopy was performed with an AVANCE AVIII 400 MHz spectrometer (Bruker, Switzerland). The spin calculation was perform by using Dmol3 software package. The SCF tolerance was 10^{-6} hartree for energy with the smearing parameter of 0.005 hartree. The DNP basis set was used to perform all electron calculations and the spin was set as unrestricted.

Conflict of interest

The authors declare no conflict of interest.

[1] a) J. H. Clark, *Acc. Chem. Res.* **2002**, *35*, 791–797; b) J. Zhang, X. Liu, R. Blume, A. Zhang, R. Schlögl, D. S. Su, *Science* **2008**, *322*, 73–77; c) Y. Li, S. Das, S. Zhou, K. Junge, M. Beller, *J. Am. Chem. Soc.* **2012**, *134*, 9727–9732.

[2] a) J. Pyun, *Angew. Chem. Int. Ed.* **2011**, *50*, 46–48; *Angew. Chem.* **2011**, *123*, 46–48; b) D. S. Su, J. Zhang, B. Frank, A. Thomas, X. Wang, J. Paraknowitsch, R. Schlögl, *ChemSusChem* **2010**, *3*, 169–180; c) M. A. Patel, F. Luo, M. R. Khoshi, E. Rabie, Q. Zhang, C. R. Flach, R. Mendelsohn, E. Garfunkel, M. Szostak, H. He, *ACS Nano* **2016**, *10*, 2305–2315; d) H. Yu, F. Peng, J. Tan, X. Hu, H. Wang, J. Yang, W. Zheng, *Angew. Chem. Int. Ed.* **2011**, *50*, 3978–3982; *Angew. Chem.* **2011**, *123*, 4064–4068.

[3] a) D. R. Dreyer, H. P. Jia, C. W. Bielawski, *Angew. Chem. Int. Ed.* **2010**, *49*, 6813–6816; *Angew. Chem.* **2010**, *122*, 6965–6968; b) P. F. Zhang, Y. T. Gong, H. R. Li, Z. R. Chen, Y. Wang, *Nat. Commun.* **2013**, *4*, 1593.

[4] J. McGregor, Z. Huang, E. P. J. Parrott, J. A. Zeitler, K. L. Nguyen, J. M. Rawson, A. Carley, T. W. Hansen, J.-P. Tessonnier, D. S. Su, *J. Catal.* **2010**, *269*, 329–339.

[5] a) H. Huang, J. Huang, Y.-M. Liu, H.-Y. He, Y. Cao, K.-N. Fan, *Green Chem.* **2012**, *14*, 930–934; b) C. Su, M. Acik, K. Takai, J. Lu, S. J. Hao, Y. Zheng, P. Wu, Q. Bao, T. Enoki, Y. J. Chabal, K. P. Loh, *Nat. Commun.* **2012**, *3*, 1298.

[6] C. Su, K. P. Loh, *Acc. Chem. Res.* **2013**, *46*, 2275–2285.

[7] H. He, M. Feng, Q. Chen, X. Zhang, H. Zhan, *Angew. Chem. Int. Ed.* **2016**, *55*, 936–940; *Angew. Chem.* **2016**, *128*, 948–952.

[8] a) D. Pan, J. Zhang, Z. Li, M. Wu, *Adv. Mater.* **2010**, *22*, 734–738; b) M. L. Mueller, X. Yan, J. A. McGuire, L. S. Li, *Nano Lett.* **2010**, *10*, 2679–2682.

[9] H. Li, C. Sun, M. Ali, F. Zhou, X. Zhang, D. R. MacFarlane, *Angew. Chem. Int. Ed.* **2015**, *54*, 8420–8424; *Angew. Chem.* **2015**, *127*, 8540–8544.

[10] Y. Han, H. Huang, H. Zhang, Y. Liu, X. Han, R. Liu, H. Li, Z. Kang, *ACS Catal.* **2014**, *4*, 781–787.

[11] a) H. Li, X. He, Z. Kang, H. Huang, Y. Liu, J. Liu, S. Lian, C. H. Tsang, X. Yang, S. T. Lee, *Angew. Chem. Int. Ed.* **2010**, *49*, 4430–4434; *Angew. Chem.* **2010**, *122*, 4532–4536; b) H. Li, R. Liu, Y. Liu, H. Huang, H. Yu, H. Ming, S. Lian, S.-T. Lee, Z. Kang, *J. Mater. Chem.* **2012**, *22*, 17470–17475; c) H. T. Li, R. H. Liu, S. Y. Lian, Y. Liu, H. Huang, Z. H. Kang, *Nanoscale* **2013**, *5*, 3289–3297.

[12] S. Y. Zhao, C. X. Li, L. P. Wang, N. Y. Liu, S. Qiao, B. B. Liu, H. Huang, Y. Liu, Z. H. Kang, *Carbon* **2016**, *99*, 599–606.

[13] J. Peng, W. Gao, B. K. Gupta, Z. Liu, R. Romero-Aburto, L. Ge, L. Song, L. B. Alemany, X. Zhan, G. Gao, *Nano Lett.* **2012**, *12*, 844–849.

[14] G. Chen, Z. Zhuo, K. Ni, N. Y. Kim, Y. Zhao, Z. Chen, B. Xiang, L. Yang, Q. Zhang, Z. Lee, X. Wu, R. S. Ruoff, Y. Zhu, *Small* **2015**, *11*, 5296–5304.

[15] Z. Zhang, J. Zhang, N. Chen, L. Qu, *Energy Environ. Sci.* **2012**, *5*, 8869–8890.

[16] a) X. H. Li, M. Antonietti, *Angew. Chem. Int. Ed.* **2013**, *52*, 4572–4576; *Angew. Chem.* **2013**, *125*, 4670–4674; b) A. Grirrane, A. Corma, H. Garcia, *Science* **2008**, *322*, 1661–1664.

[17] S. Biswas, B. Dutta, K. Mullick, C.-H. Kuo, A. S. Poyraz, S. L. Suib, *ACS Catal.* **2015**, *5*, 4394–4403.

[18] F. Su, S. C. Mathew, L. Mohlmann, M. Antonietti, X. Wang, S. Blechert, *Angew. Chem. Int. Ed.* **2011**, *50*, 657–660; *Angew. Chem.* **2011**, *123*, 683–686.

[19] a) B. Zhu, M. Lazar, B. G. Trewyn, R. J. Angelici, *J. Catal.* **2008**, *260*, 1–6; b) B. Chen, L. Wang, S. Gao, *ACS Catal.* **2015**, *5*, 5851–5876.

[20] C. D. Johnson, *The Hammett Equation*, CUP Archive, **1973**.

[21] a) J. Ye, S. Wu, K. Ni, Z. Tan, J. Xu, Z. Tao, Y. Zhu, *ChemPhysChem* **2017**, *18*, 1929–1936; b) J. C. Espinosa, S. Navalón, M. Álvaro, H. García, *ChemCatChem* **2016**, *8*, 2642–2648.

[22] M. Acik, G. Lee, C. Mattevi, A. Pirkle, R. M. Wallace, M. Chhowalla, K. Cho, Y. Chabal, *J. Phys. Chem. C* **2011**, *115*, 19761–19781.

[23] S. H. Jin, D. H. Kim, G. H. Jun, S. H. Hong, S. Jeon, *ACS Nano* **2013**, *7*, 1239–1245.

[24] F. Hu, F. Patel, F. Luo, C. Flach, R. Mendelsohn, E. Garfunkel, H. He, M. Szostak, *J. Am. Chem. Soc.* **2015**, *137*, 14473–14480.

[25] A. Lerf, H. He, M. Forster, J. Klinowski, *J. Phys. Chem. B* **1998**, *102*, 4477–4482.

[26] K. Takai, T. Suzuki, T. Enoki, H. Nishihara, T. Kyotani, *Phys. Rev. B* **2010**, *81*, 205420.

[27] O. Arias de Fuentes, T. Ferri, M. Frasconi, V. Paolini, R. Santucci, *Angew. Chem. Int. Ed.* **2011**, *50*, 3457–3461; *Angew. Chem.* **2011**, *123*, 3519–3523.

[28] F. Atamny, J. Blöcker, A. Dübotzky, H. Kurt, O. Timpe, G. Loose, W. Mahdi, R. Schlögl, *Mol. Phys.* **1992**, *76*, 851–886.

[29] a) H.-P. Jia, D. R. Dreyer, C. W. Bielawski, *Tetrahedron* **2011**, *67*, 4431–4434; b) B. Frank, J. Zhang, R. Blume, R. Schlögl, D. S. Su, *Angew. Chem. Int. Ed.* **2009**, *48*, 6913–6917; *Angew. Chem.* **2009**, *121*, 7046–7051.

[30] S. Minakata, Y. Ohshima, A. Takemiya, I. Ryu, M. Komatsu, Y. Ohshiro, *Chem. Lett.* **1997**, *26*, 311–312.

[31] F. Su, S. C. Mathew, G. Lipner, X. Fu, M. Antonietti, S. Blechert, X. Wang, *J. Am. Chem. Soc.* **2010**, *132*, 16299–16301.

[32] a) D. W. Boukhvalov, D. R. Dreyer, C. W. Bielawski, Y. W. Son, *ChemCatChem* **2012**, *4*, 1844–1849; b) L. Liu, Y. P. Zhu, M. Su, Z. Y. Yuan, *ChemCatChem* **2015**, *7*, 2765–2787.

[33] D. R. Dreyer, C. W. Bielawski, *Chem. Sci.* **2011**, *2*, 1233–1240.